The collection of review articles

Progress in Earth and Planetary Science

PEPS

(The 5th Edition: Published from 2023 to 2025)

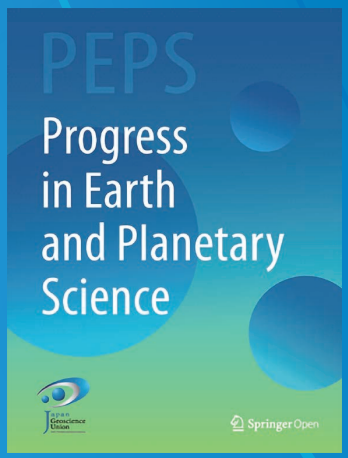

Japan Geoscience Union（JpGU）Open Access journal

https://link.springer.com/journal/40645

CONTENTS

Biogeosciences

Interdisciplinary research

Progress in Earth and Planetary Science
https://progearthplanetsci.org/en/

Review articles : Space and planetary sciences

Space and atmospheric physics on Svalbard: a case for continued incoherent scatter radar measurements under the cusp and in the polar cap boundary region

Lisa Baddeley, Dag Lorentzen, Stein Haaland, Erkka Heino, Ingrid Mann, Wojciech Miloch, Kjellmar Oksavik, Noora Partamies, Andres Spicher, Juha Vierinen

Keywords: Ionosphere, Atmospheric science, Space weather, Cusp, Polar cap, Plasma turbulence, Space debris, Incoherent scatter radar, Atmospheric escape

Incoherent scatter radars (ISRs) represent the only instrument (both ground and space based) capable of making high temporal and spatial resolution measurements of multiple atmospheric parameters—such as densities, temperatures, particle velocities, mass flux—over an altitude range covering the entire mesosphere/lower thermosphere/ionosphere (MLTI) system on a quasi-continuous basis. The EISCAT Svalbard incoherent scatter radar (ESR), located just outside Longyearbyen (78.15°N) on Svalbard, is the only currently operating facility capable of making such measurements inside the polar cusp—an area of significant energy input into the atmosphere and characterized by heating instabilities and turbulence. The ESR was built in the mid-1990s and has provided valuable data for the international experimental and modelling communities. New radar technologies are now available, in the form of phased array systems, which offer new data products and operational flexibility. This paper outlines the achievements and current research focus of the ESR and provides scientific arguments, compiled from inputs across the international scientific community, for a new phased array ISR facility on Svalbard. In addition to the fundamental scientific arguments, the paper discusses additional benefits of continued ISR observations on Svalbard, building on the key findings of the ESR. Svalbard has a large network of complementary instrumentation both focused on the MLTI system (e.g. the Kjell Henriksen auroral Observatory, the Svalbard SuperDARN radar and the Svalrak sounding rocket launch facility) with synergies to other research fields, such as meteorology and oceanography. As a further holistic system science view of the Earth becomes more important, a new ISR on Svalbard will be important also in this respect with its ability to provide datasets with a wide range of scientific applications. Increased activity in space has highlighted problematic issues such as space debris. A changing Arctic has also seen increased human activity via the opening up of new shipping routes, which are reliant on GNSS technology that is effected by severe turbulence in the MLTI system. As such, societal applications of a future ISR are also presented. The accessibility and logistical support for such a facility is also briefly discussed..

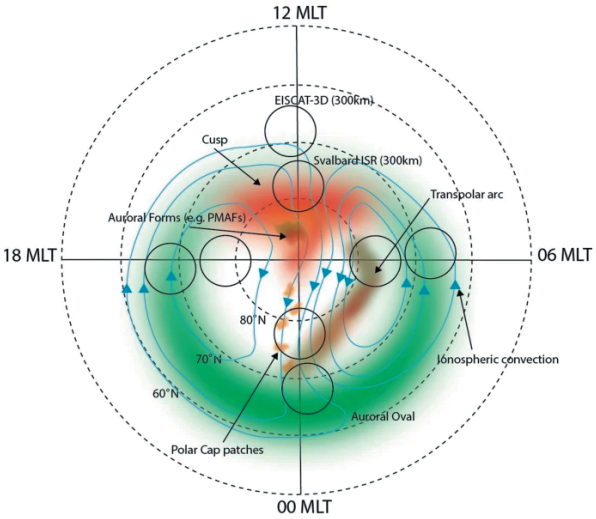

Published: 2023/9/4
https://doi.org/10.1186/s40645-023-00585-9

Progress in Earth and Planetary Science
https://progearthplanetsci.org/en/

Review articles : Atmospheric and hydrospheric sciences

Climate-relevant properties of black carbon aerosols revealed by in situ measurements: a review

Nobuhiro Moteki

Keywords: Atmospheric chemistry, Atmospheric radiation, Climate, Aerosol, Light-absorbing aerosols, Black carbon

Light-absorbing aerosols affect atmospheric radiation, dynamics, and precipitations through shortwave absorption in the atmosphere and snowpack. Black carbon (BC) is considered the most significant contributor to global shortwave absorption among all the known light-absorbing aerosol components. In analyses and predictions of BC's lifecycle and climate effects, multiscale field observations are needed to test the fundamental assumptions in the climate model. In situ measurements, the focus of this review, fill the gap of observational information accessible from remote sensing and laboratory analyses. This article reviews historical backgrounds, recent advances in in situ measurements of BC, and the resulting observational findings used to update the assumptions in climate models and remote sensing. Finally, we raise open problems that demand a rethinking and future investigation.

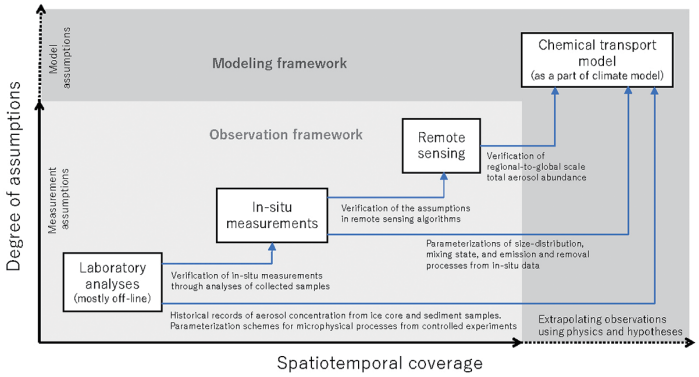

Figure 1. Roles and relationships of the four-different approaches in aerosol-climate research. Laboratory analyses of collected samples, in-situ measurements, and remote sensing provide complementary observational information needed for reducing assumptions in the atmospheric chemical transport model (sub-module of the climate model).

Illustrating the physical principle of detecting the light-absorbing black carbon and iron oxidesaerosol particles using the single-particle laser-induced incandescence

Published: 2023/3/6
https://doi.org/10.1186/s40645-023-00544-4

Progress in Earth and Planetary Science
https://progearthplanetsci.org/en/

Review articles : Atmospheric and hydrospheric sciences

Greenhouse gases observing satellite 2 (GOSAT-2): Mission overview

Ryoichi Imasu, Tsuneo Matsunaga, Masakatsu Nakajima, Yukio Yoshida, Kei Shiomi, Isamu Morino, Naoko Saitoh, Yosuke Niwa, Yu Someya, Yu Oishi, Makiko Hashimoto, Hibiki Noda, Kouki Hikosaka, Osamu Uchino, Shamil Maksyutov, Hiroshi Takagi, Haruma Ishida, Takashi Y. Nakajima, Teruyuki Nakajima & Chong Shi

Keywords: GOSAT-2, GOSAT, Carbon dioxide, Methane, Carbon monoxide, Black carbon, Solar-induced, chlorophyll fluorescence, TANSO-FTS-2, TANSO-CAI-2, Intelligent pointing mechanism

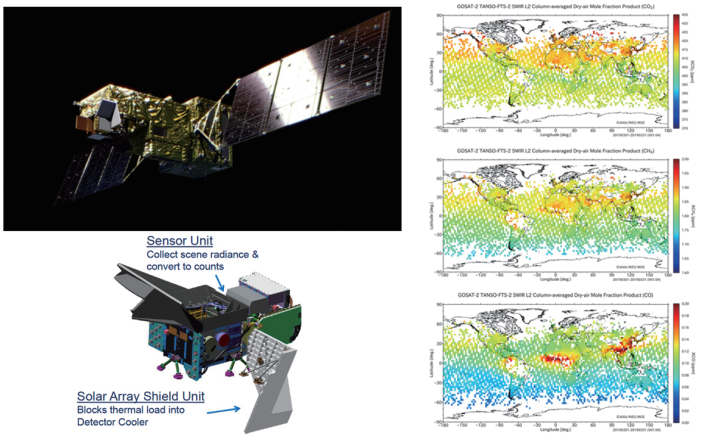

Artistic image of GOSAT-2 in orbit (left-top), schematic image of the TANSO-FTS-2 sensor (left-bottom). Examples of observed column-averaged dry-air mole fraction products of CO_2 (right-top), CH_4 (right-middle), and CO (right-bottom). Values are averaged in each 2.5° mesh area for March 2019.

The Greenhouse gases Observing SATellite 2 (GOSAT-2) was launched in October 2018 as a successor to GOSAT (launched in 2009), the first satellite to specialize in greenhouse gas observations. Compared to the GOSAT sensors, the sensors of GOSAT-2 offer higher performance in most respects. The quality and quantity of data from observations are expected to be improved accordingly. The signal-to-noise ratio (SNR) is better in both the SWIR and TIR bands of TANSO-FTS-2, which is the main sensor of GOSAT-2. This improvement ultimately enhances the accuracy of greenhouse gas concentration analysis. Furthermore, because of the improved SNR in the SWIR band, the northern limit at which data are obtainable in high-latitude regions of the Northern Hemisphere in winter, where observation data have remained unavailable because of weak signal strength, has moved to higher latitudes. As better data are obtained in greater quantities, progress in carbon cycle research for high-latitude regions is anticipated. Moreover, the improvement of SNR in the TIR band is expected to be considerable. Particularly, the resolutions of the vertical concentration distributions of CO2 and CH4 have been improved drastically. The first function introduced for GOSAT-2 that is not in GOSAT is an intelligent pointing mechanism: a cloud area avoidance function using the in-field camera of TANSO-FTS-2. This function can increase the amounts of observation data globally and can improve the accuracy of CO2 emissions estimation and measurements of uptake intensity. The effects are expected to be strong, especially for the tropics because cumulus clouds are the most common cloud type. The intelligent pointing system can avoid the clouds effectively. Another important benefit of TANSO-FTS-2 is that the wavelength range of Band 3 of SWIR has been expanded for measuring carbon monoxide (CO). Because CO originates from combustion, it is used to evaluate some effects of human activities in urban areas and biomass burning in fields. Particularly, black carbon-type aerosols can be measured by the sub-sensor, TANSO-CAI-2, to assess biomass burning along with CO2 and CO by TANSO-FTS-2.

Published: 2023/7/3
https://doi.org/10.1186/s40645-023-00562-2

Progress in Earth and Planetary Science
https://progearthplanetsci.org/en/

Review articles : Atmospheric and hydrospheric sciences

Recent global nonhydrostatic modeling approach without using a cumulus parameterization to understand the mechanisms underlying cloud changes due to global warming

Akira T. Noda, Tomoki Ohno, Chihiro Kodama, Ying-Wen Chen, Naomi Kuba, Tatsuya Seiki, Yohei Yamada, Masaki Satoh

Keywords: Clouds, Global nonhydrostatic model, Global warming, High-resolution climate simulation, Model improvement

Clouds are the primary source of uncertainty in the prediction of climate change. To reduce the uncertainty of cloud simulations and overcome this difficulty in prediction, many climate modeling centers are now developing a new type of climate model, the global nonhydrostatic atmospheric model, which reduces the uncertainty arising from a cumulus parameterization by computing clouds explicitly using a cloud microphysics scheme. Among the global nonhydrostatic atmospheric models used in recent intercomparison studies, NICAM aims to project climate change by improving our understanding of cloud changes due to warming and related physical processes. NICAM is the first global nonhydrostatic model and was developed by our research team. This review summarizes the outcomes of a recent major five-year research program in Japan for studying climate using NICAM, as well as providing an overview of current issues regarding the use of global kilometer-scale simulations in high-resolution climate modeling.

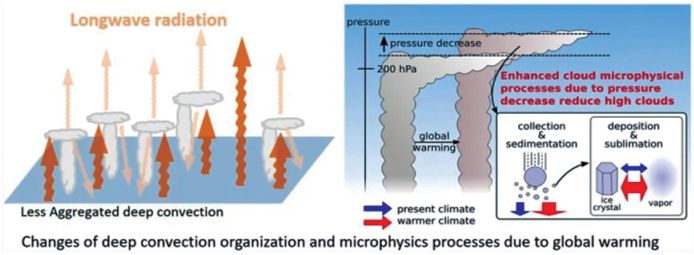

Changes of deep convection organization and microphysics processes due to global warming

Published: 2023/8/18
https://doi.org/10.1186/s40645-023-00583-x

Progress in Earth and Planetary Science
https://progearthplanetsci.org/en/

Review articles : Atmospheric and hydrospheric sciences

Basal emission rates of isoprene and monoterpenes from major tree species in Japan: interspecies and intraspecies variabilities

Akira Tani, Noboru Masui, Ting-Wei Chang, Motonori Okumura, Yutaka Kokubu

Keywords: Tower flux measurement, Flow-through chamber, Static chamber, Temperature, Light intensity, Quercus, Bamboo

Uncontrolled terpenoid emissions from forest trees in Japan may have contributed to high O_3 concentrations observed in urban and suburban areas. To estimate ozone formation via a series of reactions between NO_x and terpenoids using atmospheric chemistry models, it is important to produce terpenoid emission inventories by collecting all reported emission data for the major tree species in Japan and examining their reliability. In this review, we first describe three different plant terpenoid emission types, i.e., isoprene-emitting type, monoterpene-emitting type with storage tissues and organs, and monoterpene-emitting type without storage tissues and organs. Second, we describe various methods for measuring plant terpenoid emissions, including a recently developed simplified method, and explain their reliability. We emphasized that applicable measurement methods depend on the terpenoid emission types. Data obtained using static chamber methods should not be considered because they have the highest uncertainty resulting from normal chamber materials that are not specific to terpenoid measurements and lack humidity control. Finally, we show the absolute values of the collected emission rates and describe their variability. The deciduous oak species, *Quercus serrata* and *Quercus mongolica* var. *crispula*, and bamboo species, *Phyllostachys pubescens* and *Phyllostachys bambusoides*, are strong isoprene emitters. Among the monoterpene emitters, four evergreen broadleaf trees, including three *Quercus* species, had the highest basal emission rate (BER). The monoterpene storage type conifers *Larix kaempferi* and *Pinus densiflora* have relatively lower BERs. Emission data are not available for *Castanopsis cuspidata,* and seasonal changes in emission rates have not been reported for several major tree species in the top 20 rankings. Within species, the reported emission rates of some tree species differed by threefold. These differences may be attributed to the reliability of the measurement and analytical systems, tree age, leaf morphology, environmental conditions, and genetic diversity. We emphasize the need for reliable measurements to achieve a more precise terpenoid emission inventory for major tree species in Japan.

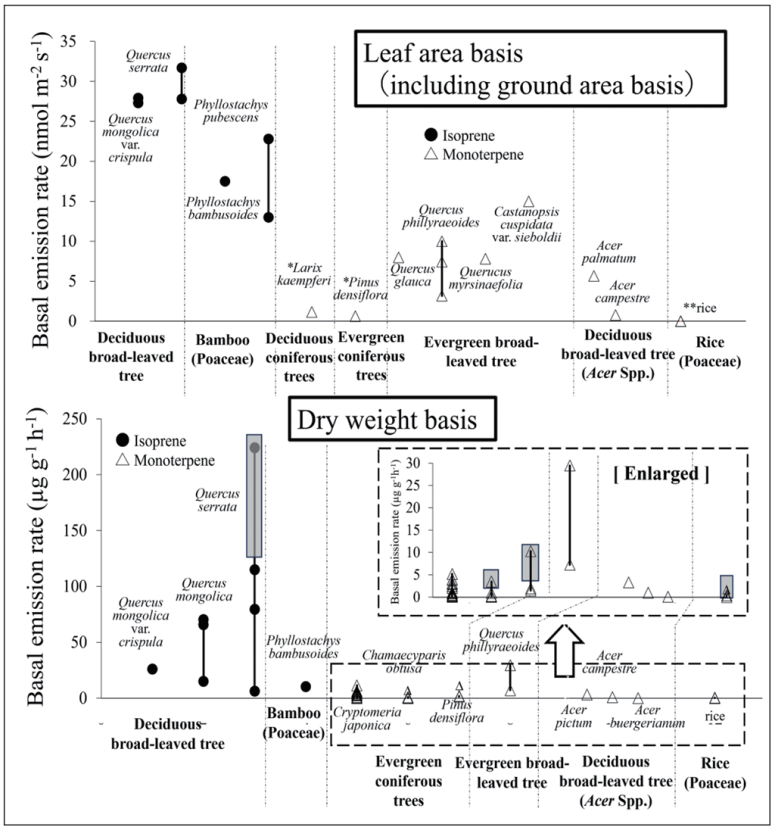

Basal emission rates (BERs) of isoprene and total monoterpenes from major plant species in Japan. Upper and lower panels show BERs on leaf area basis and dry weight basis, respectively. Dots show the BERs collected in summer season in individual reports.

Published: 2024/7/30
https://doi.org/10.1186/s40645-024-00645-8

Progress in Earth and Planetary Science
https://progearthplanetsci.org/en/

Review articles : Atmospheric and hydrospheric sciences

Achievements in atmospheric sciences by the large-ensemble and high-resolution forecasting studies using the supercomputer Fugaku

Masaki Satoh, Takuya Kawabata, Tomoki Miyakawa, Masuo Nakano, Hisashi Yashiro, Takemasa Miyoshi, Le Duc, Pin-Ying Wu, Tsutao Oizumi, Yasumitsu Maejima, James Taylor, Ryoichi Yoshimura, Koji Terasaki, Yohei Yamada, Ryusuke Masunaga, Takao Kawasaki, Masahiro Tanoue

Keywords: Fugaku, High-resolution atmospheric simulations, Ensemble simulations, Numerical weather forecasting, Probabilistic prediction, Extreme weather events, Disaster prevention, Meso-scale modeling, Observational big data, Trace gas transport

This article reviews the outcomes of a three-year project utilizing “Fugaku,” Japan’ s flagship supercomputer, to conduct high-resolution ensemble simulations using atmosphere or atmosphere–ocean coupled models for both the Japan region and the entire globe. The project name was “Large Ensemble Atmospheric and Environmental Prediction for Disaster Prevention and Mitigation.” The primary objective is to enhance the accuracy of numerical weather forecasting and provide probabilistic prediction information. To address the increasing severity of extreme weather events associated with global warming, such as torrential rainfall and tropical cyclones, high-resolution large-number ensemble atmospheric forecasting experiments have been conducted across timescales ranging from a few minutes to several weeks, extending to seasonal scales. This project aims to investigate advanced methodology using high-performance computing that provides probabilistic forecasts with sufficient lead time for effective disaster prevention and mitigation. Three sub-themes are explored: 1. meso-scale and regional modeling studies; 2. global and seasonal to sub-seasonal studies; and 3. innovative approaches to environmental studies. Central to this effort are high-resolution simulations that accurately represent cumulonimbus clouds and meso-scale systems, which are crucial for predicting severe weather phenomena alongside improved initial conditions derived from observational big data. These advancements are essential for predicting meteorological disasters caused by extreme events. Furthermore, the integration of probability information with improved accuracy significantly enhances disaster risk management, thereby increasing the practical utility of forecasts. This research also aims to develop pioneering innovative numerical weather and atmospheric environment forecasting technologies by incorporating big data from trace gas observations in addition to conventional meteorological data.

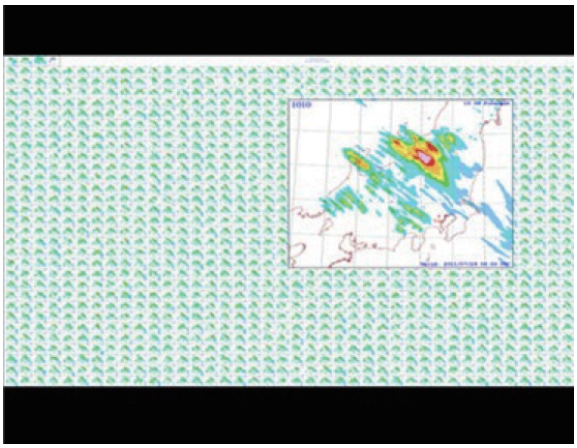

The figure shows an example of a thousand-member ensemble forecast for the torrential rainfall that occurred on July 4, 2020, in southern Kumamoto.

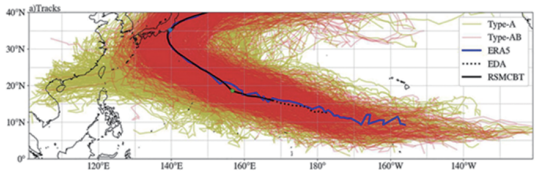

Simulated tracks of Faxai-like vortices in the Faxai large-ensemble simulation. The red and yellow lines, respectively, show the tracks of the vortices that approached Japan similarly to reality (denoted as Type-AB), and vortices that were generated similarly to reality but with large errors in the tracks (denoted as Type-A). After Fig. 1 of Yamada et al. (2024).

Published: 2025/8/6
https://doi.org/10.1186/s40645-025-00730-6

Progress in Earth and Planetary Science
https://progearthplanetsci.org/en/

Review articles : Solid earth sciences

A review on slow earthquakes in the Japan Trench

Tomoaki Nishikawa, Satoshi Ide, Takuya Nishimura

Keywords: Japan Trench ,Slow earthquake, Tectonic tremor, Very-low-frequency earthquake, Slow slip event, Megathrust earthquake, Tohoku-Oki earthquake, Subduction zone, Crustal structure, Geological environment

Slow earthquakes are episodic slow fault slips. They form a fundamental component of interplate deformation processes, along with fast, regular earthquakes. Recent seismological and geodetic observations have revealed detailed slow earthquake activity along the Japan Trench—the subduction zone where the March 11, 2011, moment magnitude (M_w) 9.0 Tohoku-Oki earthquake occurred. In this paper, we review observational, experimental, and simulation studies on slow earthquakes along the Japan Trench and their research history. By compiling the observations of slow earthquakes (e.g., tectonic tremors, very-low-frequency earthquakes, and slow slip events) and related fault slip phenomena (e.g., small repeating earthquakes, earthquake swarms, and foreshocks of large interplate earthquakes), we present an integrated slow earthquake distribution along the Japan Trench. Slow and megathrust earthquakes are spatially complementary in distribution, and slow earthquakes sometimes trigger fast earthquakes in their vicinities. An approximately 200-km-long along-strike gap of seismic slow earthquakes (i.e., tectonic tremors and very-low-frequency earthquakes) corresponds with the huge interplate locked zone of the central Japan Trench. The M_w 9.0 Tohoku-Oki earthquake ruptured this locked zone, but the rupture terminated without propagating deep into the slow-earthquake-genic regions in the northern and southern Japan Trench. Slow earthquakes are involved in both the rupture initiation and termination processes of megathrust earthquakes in the Japan Trench. We then compared the integrated slow earthquake distribution with the crustal structure of the Japan Trench (e.g., interplate sedimentary units, subducting seamounts, petit-spot volcanoes, horst and graben structures, residual gravity, seismic velocity structure, and plate boundary reflection intensity) and described the geological environment of the slow-earthquake-genic regions (e.g., water sources, pressure–temperature conditions, and metamorphism). The integrated slow earthquake distribution enabled us to comprehensively discuss the role of slow earthquakes in the occurrence process of the Tohoku-Oki earthquake. The correspondences of the slow earthquake distribution with the crustal structure and geological environment provide insights into the slow-earthquake-genesis in the Japan Trench and imply that highly overpressured fluids are key to understanding the complex slow earthquake distribution. Furthermore, we propose that detailed monitoring of slow earthquake activity can improve the forecasts of interplate seismicity along the Japan Trench.

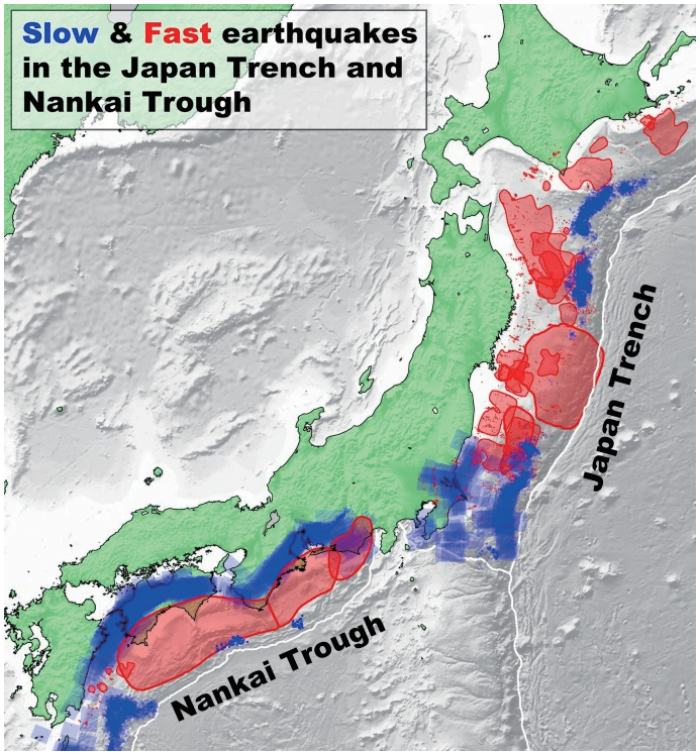

Distribution of slow and fast (regular) earthquakes in the Japan Trench and Nankai Trough. Blue and red symbols indicate areas where slow and fast earthquakes occur, respectively.

Published: 2023/1/3
https://doi.org/10.1186/s40645-022-00528-w

Progress in Earth and Planetary Science
https://progearthplanetsci.org/en/

Review articles : Solid earth sciences

Significance of the high-pressure properties and structural evolution of gas hydrates for inferring the interior of icy bodies

Hisako Hirai, Hirokazu Kadobayashi

Keywords: Methane hydrate, Hydrogen hydrate, High-pressure properties, High and low temperatures, Structural evolution, Transition mechanism, Guest orientational ordering, Molecular dissociation, Icy bodies, Diamond-anvil cell (DAC)

Hydrogen, methane, and water ice are among the most abundant materials in the universe. Based on experimental, theoretical, and spacecraft data, gas hydrates consisting of gas and water ice have been predicted to exist throughout the universe. This review discusses the high-pressure properties of two common gas hydrates (methane and hydrogen hydrates) at low and high temperatures based primarily on experimental results. Gas hydrates consist of a water molecule host and a gaseous guest. They have a clathrate structure at low pressure and a filled-ice structure at high pressure. The host encloses the guest, and a specific interaction occurs between the guest and host, resulting in unique physical properties. When subjected to pressure, gas hydrates undergo various phase changes. Based on pressure and guest size, a general rule for phase changes occurring in gas hydrates exists. Analysis of the phase-transition mechanism shows that some cages are maintained after the transition to the next clathrate structure, while others are recombined into different cages of the next structure. This is a novel mechanism that can be called “cage recombination mechanism.” Low-temperature and high-pressure experiments have revealed that as the pressure increases, the guest molecules undergo a stepwise progression of orientational ordering, i.e., restriction of free rotation, which induces structural changes that stabilize the structure at high pressure. Theoretical studies have predicted that hydrogen-bond symmetrization in the host occurs at even higher pressures, further stabilizing the structure. Thus, hydrates respond to environmental changes such as pressure to achieve self-organization by the orientational ordering of the guest and hydrogen-bond symmetrization of the host. Additionally, results of high-temperature and high-pressure experiments conducted at conditions comparable to those in Neptune’s ice mantle show that methane hydrate decomposes into solid methane and ice VII, both of which melt at further elevated temperatures. Then, the methane molecules undergo further molecular dissociation to form diamonds. These findings are valuable for modeling the interiors of icy planets and understanding how magnetic fields and heat are generated.

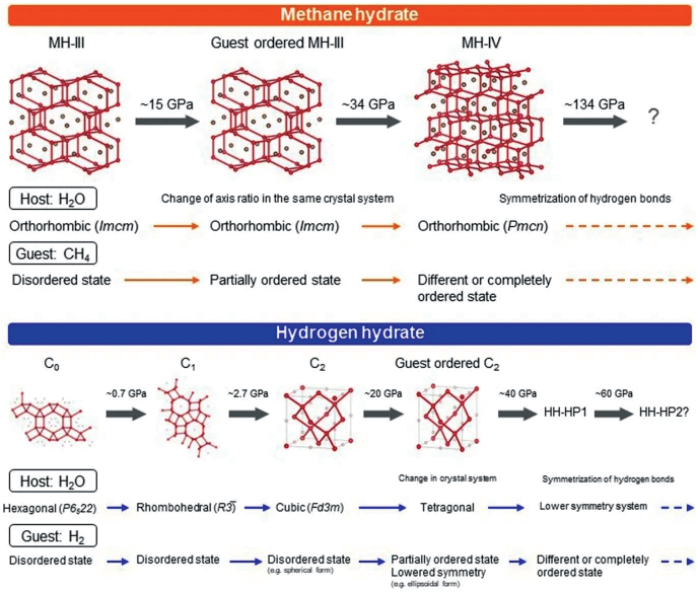

An overview of the structural evolution of (top) MH and (bottom) HH after transition to the filled-ice structure, except for HH-C0. With increasing pressure, the guests undergo stepwise orientational ordering accompanied by structural changes. Hydrogen-bond symmetrization of the host was predicted to occurs at even higher pressures.

Published: 2023/1/13
https://doi.org/10.1186/s40645-023-00534-6

Progress in Earth and Planetary Science
https://progearthplanetsci.org/en/

Review articles : Solid earth sciences

Heterogeneous rheology of Japan subduction zone revealed by postseismic deformation of the 2011 Tohoku-oki earthquake

Sambuddha Dhar, Jun Muto, Yusaku Ohta, Takeshi Iinuma

Keywords: Postseismic deformation, GNSS observations, viscoelastic relaxation, afterslip, nonlinear rheology, earthquake deformation cycle, rheological heterogeneity

The 2011 Tohoku-oki earthquake produced the most well-recorded postseismic deformation of any megathrust earthquake in the world. Over the last decade, researchers have used a dense and widespread geodetic network of more than 1300 Global Navigation Satellite System (GNSS) stations inland, as well as the about 50 stations on the seafloor, to investigate the various deformation sources responsible for the observed crustal deformation. One of the contributing mechanisms to this crustal deformation is the stress relaxation of the viscoelastic mantle beneath the Japanese arc. As evident in experimental rock physics and geophysical observations, ambient mantle conditions and related rheology are expected to be heterogeneous in space. However, the contribution of such rheological heterogeneities to the postseismic deformation is still poorly understood. Here, we piece together several rheological heterogeneities inferred from the decade-long postseismic deformation of the 2011 Tohoku-oki earthquake. We reviewed more than twenty postseismic models to understand how viscoelastic earth can influence the postseismic surface deformation observed after the Tohoku-oki earthquake. Besides, we employed several synthetic models to tease out the contribution of individual rheological heterogeneities such as depth-dependent rheology of mantle wedge, oceanic asthenosphere, and low-viscosity zone beneath the volcanic front. We demonstrate that the vertical postseismic observation is the key to unravel rheological complexity beneath northeastern Japan. The broader vertical deformation pattern reveals the major viscosity contrast between backarc and forearc, and small-scale subsidence detects the presence of low-viscosity bodies related to arc magmatism. In short, this review paper provides a vista of three-dimensional heterogeneous rheology of viscoelastic earth. These rheological heterogeneities may play a crucial role in bridging the gap between our understanding of different phase of subduction zone earthquake cycle.

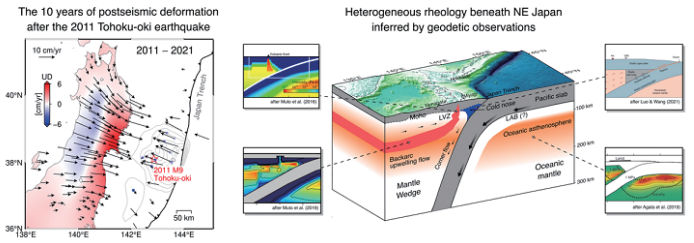

Post-seismic deformation observations for 10 years after the Tohoku offshore earthquake (left), and the heterogeneous rheological structure estimated from them (right).

Published: 2023/2/28
https://doi.org/10.1186/s40645-023-00539-1

Progress in Earth and Planetary Science
https://progearthplanetsci.org/en/

Review articles : Solid earth sciences

Progress and application of the synthesis of trans-oceanic tsunamis

Shingo Watada

Keywords: Trans-oceanic tsunami, Historical tsunamis recorded in tide gauge, Tsunami in the gravitationally coupled Earth system, Tsunami phase delay, Tsunami traveltime delay, Tsunami in the eformable Earth, Earthquake fault parameters studied by tsunami waveforms, Tsunami simulation by the phase correction method, Eulerian and Lagrangian variables, Free oscillation and forced oscillation of the Earth with an ocean layer, Compressible density-stratifed ocean

Abundant high-quality distant tsunami records from the 2010 Maule (Chile) and 2011 Tohoku-Oki earthquakes have revealed two distinctive features compared to long-wave tsunami simulations. The records show that the traveltime delay of the tsunami increases with distance from the earthquakes, and the initial phase reversal of tsunamis appears and grows systematically. The conventional tsunami theory cannot explain the observed waveforms and traveltimes of distant tsunamis, leading to the need for a new theory to explain and synthesize distant tsunamis. The propagating elevated sea surface of a tsunami compresses seawater and deforms the seafloor and the solid Earth. A propagating tsunami changes the mass distribution of the Earth and results in a spatiotemporal change in gravity, thereby altering the propagating tsunami itself. Incorporating these physics, we developed a new tsunami propagation theory in which a tsunami is naturally treated as a wave in a gravitationally and elastically coupled Earth system composed of solid Earth layers and an ocean layer. Two distinct tsunami simulation techniques based on the new tsunami propagation theory were introduced and confirmed to produce nearly identical tsunami waveforms. One technique treats tsunamis as free waves within a deformable Earth system, while the other treats tsunamis as external pressure and gravitational forces acting on the surface of a deformable Earth system. With the new techniques, the waveform and traveltime differences between the observed and simulated distant tsunamis disappear. Past distant tsunamis recorded by coastal tide gauges, which were not previously studied due to the traveltime and waveform mismatch problems, have become the focus of quantitative tsunami studies analyzing waveforms. New tsunami propagation techniques have been applied to the analysis of distant tsunami waveforms from the past 19 events and have helped to unveil the slip distributions of the past large earthquakes and to determine the earthquake origin time of the trans-Pacific tsunami events recorded by tide gauges since 1854.

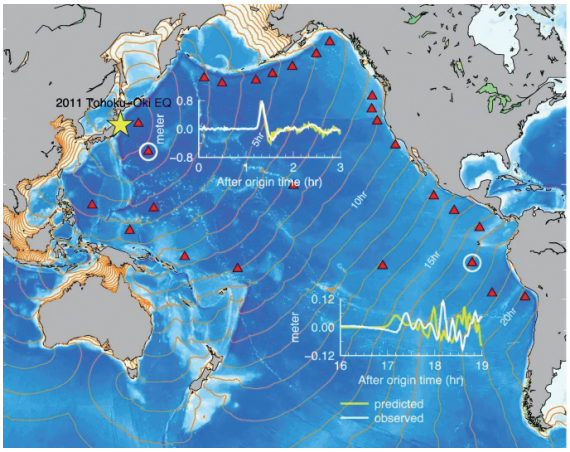

The tsunami generated by the 2011 Tohoku-Oki earthquake took almost a day to cross the Pacific Ocean, and its details were recorded by the tsunami stations (red triangle) installed on the deep seafloor. The observed tsunami (white line) and the predicted tsunami based on the classic linear long-wave theory (yellow line) are compared at the two stations circled in white.

Published: 2023/5/22
https://doi.org/10.1186/s40645-023-00555-1

Progress in Earth and Planetary Science
https://progearthplanetsci.org/en/

Review articles : Solid earth sciences

Si- versus Mg-metasomatism at the crust–mantle interface: Insights from experiments, natural observations and geochemical modeling

Atsushi Okamoto, Ryosuke Oyanagi

Keywords: Element mobility, Metasomatism, Crust–mantle interface, Fluid, Chloritization

The slab–mantle interface in subduction zones is one of the geological boundaries with the most significant chemical potential gradients, which leads to fluid-mediated metasomatic reactions and chemical transport. As subducting sediment and basaltic crust often contain silica in various forms, the Si-metasomatism of mantle rocks is thought to occur along the subduction zone interface. However, growing evidence from the geochemistry of altered rocks and thermodynamic modelling has revealed the presence of multi-component fluids at the slab interface. Here, we review the laboratory experiments, geochemical models, and natural observations that improve our understanding of mass transport and metasomatic reactions at the crust–mantle interface, focusing on the relative mobility of Mg and Si. Hydrothermal experiments using analogues for the boundary between mantle (olivine) and crust (quartz or plagioclase) under vapor-saturated pressures indicate that Si is preferentially transported from crust to mantle, whereas Mg is immobile. This result is consistent with the distribution of talc rocks in oceanic lithosphere. On the other hand, at the contact between ultramafic (e.g., serpentinite) and crustal (pelitic schist or basaltic rocks) rocks in high-pressure metamorphic terranes, a large volume of chlorite rocks form in the crustal rocks, and the volume of chlorite often exceeds talc in serpentinites. Geochemical modeling reveals that in the shallow part of a subduction zone, the dissolved Si content of fluids in equilibrium with pelitic schist ($C_{Si,crust}$) is significantly higher than the dissolved Mg content of fluids in equilibrium with mantle peridotite ($C_{Mg,mantle}$); however, $C_{Mg,mantle}$ becomes dominant at depth, resulting in the Mg-metasomatism of crustal rocks to form chlorite rocks. This Mg-metasomatism is more widespread in warmer subduction zones (e.g., the Nankai and Cascadia subduction zones) than in colder subduction zones (e.g., in Northeast Japan). In addition, the infiltration of CO_2-bearing fluid can form talc (along with carbonates) in ultramafic rocks without Si-metasomatism. Variations in the relative mobility of Si and Mg at the subduction zone interface produce variations in the overall solid volume change of mantle (expansion or contraction), the types of sheet silicates (talc versus chlorite), and the fluid budget (dehydration or hydration) during metasomatic reactions, which affects the pore fluid pressure, frictional strength of the subduction megathrust, and the location of seismicity around the mantle wedge corner.

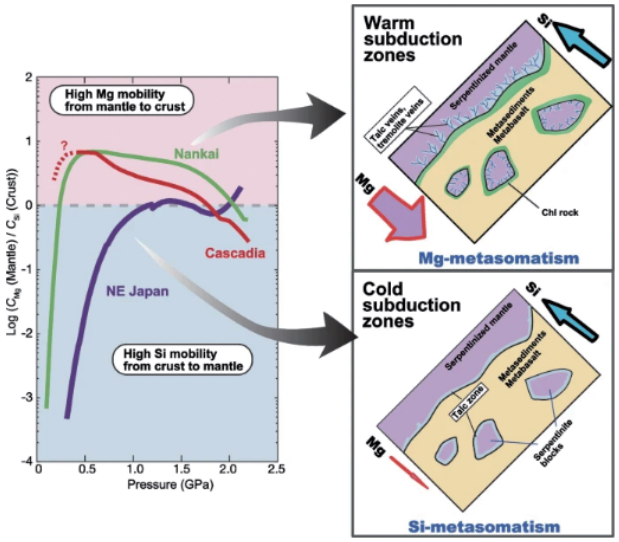

Results of geochemical modeling showing the relative mobility of Mg and Si along the geotherm of the representative subduction zones (left panel) and schematic illustrations of Si- and Mg-metasomatism at the crust-mantle interfaces within the warm (right top) and cold subduction zones (right bottom).

Published: 2023/7/18
https://doi.org/10.1186/s40645-023-00568-w

Progress in Earth and Planetary Science
https://progearthplanetsci.org/en/

Review articles : Solid earth sciences

An introductory review of the thermal structure of subduction zones: I—motivation and selected examples

Peter E. van Keken, Cian R. Wilson

Keywords: Geodynamics, Plate tectonics, Finite element methods, Subduction zone metamorphism, Arc volcanism

The thermal structure of subduction zones is fundamental to our understanding of physical and chemical processes that occur at active convergent plate margins. These include magma generation and related arc volcanism, shallow and deep seismicity, and metamorphic reactions that can release fluids. Computational models can predict the thermal structure to great numerical precision when models are fully described but this does not guarantee accuracy or applicability. In a trio of companion papers, the construction of thermal subduction zone models, their use in subduction zone studies, and their link to geophysical and geochemical observations are explored. In part I, the motivation to understand the thermal structure is presented based on experimental and observational studies. This is followed by a description of a selection of thermal models for the Japanese subduction zones.

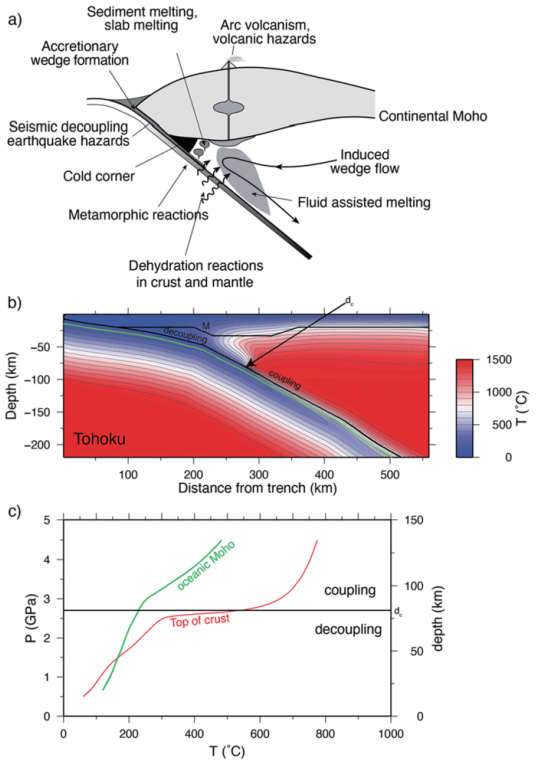

Subduction zone processes and example of thermal structure. a Cartoon of subduction zone processes (modified from van Keken (2003)). b Thermal structure predicted for Tohoku subduction (van Keken et al. (2012)). c Temperature of the top of the oceanic crust (in red) and oceanic Moho (in green) as a function of lithostatic pressure P and depth.

Published: 2023/7/28
https://doi.org/10.1186/s40645-023-00573-z

Progress in Earth and Planetary Science
https://progearthplanetsci.org/en/

Review articles : Solid earth sciences

Progress in modeling the Tohoku-oki megathrust earthquake cycle and associated crustal deformation processes

Bunichiro Shibazaki

Keywords: 2011 Tohoku-oki earthquake, Numerical modeling, Megathrust earthquake cycle, Hierarchical asperity model, Dynamic weakening, Postseismic deformation, Viscoelastic relaxation, Postseismic slip, Long-term vertical deformation

This paper summarizes the results of 10 years of research on models of the megathrust earthquake cycles and crustal deformation associated with the 2011 Tohoku-oki earthquake. Several earthquake cycle models have been proposed for the northeast Japan subduction zone to elucidate why megathrust earthquakes occur at intervals of approximately 600 years and why large slips occurred in the shallow subduction zone. A model that considers a strong asperity in the shallow plate interface, and a hierarchical asperity model that considers the scale dependence of the critical displacement of the rate- and state-dependent friction law have been proposed. Modeling with dynamic weakening of faults has also been proposed. In the model using the shallow friction characteristics obtained by the Japan Trench Fast Drilling Project, rupture from depth can propagate to the trench, resulting in shallow large slips. Submarine crustal deformation has been observed for the first time in addition to dense observations of the inland crustal deformation. The observation of the seafloor deformation near the trench showed that viscoelastic relaxation played an important role in short-term postseismic deformation near the trench. The effects of the low-viscosity region at the oceanic lithosphere and asthenosphere boundary, and the cold forearc mantle wedge (cold nose) have been discussed. Simulations using the nonlinear flow law of rock in the mantle, where a power–law relationship holds between stress and strain rate, and the fault friction law at the plate boundary, show that the Tohoku-oki earthquake caused large stress fluctuations, resulting in a sudden viscosity decrease and rapid flow in the asthenosphere below the oceanic lithosphere. The simulations of the crustal deformation associated with the Tohoku-oki earthquake cycle also indicate that in the later stage of the earthquake cycle, the Pacific coastal region begins to subside due to the increasing slip deficit rate on the deeper parts of the plate interface. These results explain the subsidence of the Pacific coast of northeast Japan observed for about 100 years prior to the Tohoku-oki earthquake. In the future, a model that explains the long-term crust and mantle deformation during the entire Tohoku-oki earthquake cycle must be constructed.

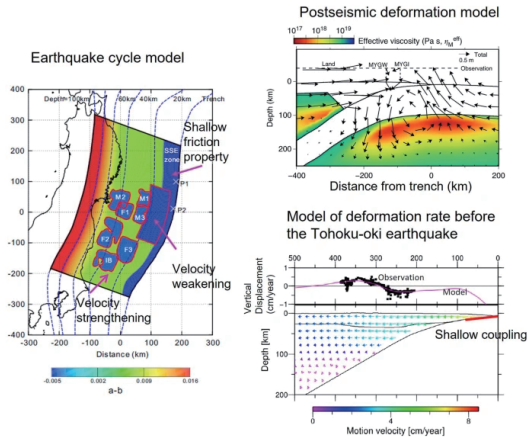

Examples of modeling of megathrust earthquake cycles and postseismic deformation for the 2011 Tohoku-oki earthquake and long-term vertical crustal deformation prior to the Tohoku-oki earthquake presented in this paper. (Left) Distribution of friction parameters used in the earthquake cycle model (Shibazaki et al. 2019), considering shallow fault friction properties obtained from JFAST. Regions, where a-b is negative, indicate asperities of velocity weakening. (Right top) Modeling of postseismic deformation (Agata et al. 2019). Total displacement of the crust and mantle and viscosity of the mantle 2.8 years after the Tohoku-oki earthquake. The Tohoku-oki earthquake caused large stress fluctuations, resulting in a sudden viscosity decrease and rapid flow in the asthenosphere below the oceanic lithosphere. (Right bottom) Modeling of vertical crustal deformation rates and motions in the island arc crust and mantle prior to the Tohoku-oki earthquake (Sasajima et al. 2019). The model reproduced the subsidence of the Pacific coast of northeast Japan observed for about 100 years prior to the Tohoku-oki earthquake.

Published: 2023/7/31
https://doi.org/10.1186/s40645-023-00575-x

Progress in Earth and Planetary Science
https://progearthplanetsci.org/en/

Review articles : Solid earth sciences

The nature of the Pacific plate as subduction inputs to the northeastern Japan arc and its implication for subduction zone processes

Gou Fujie, Shuichi Kodaira, Koichiro Obana, Yojiro Yamamoto, Takehi Isse, Tomoaki Yamada, Tetsuo No, Yasuyuki Nakamura, Seiichi Miura

Keywords: Incoming oceanic plate, Oceanic crust, Controlled-source seismic survey, Japan Trench, Outer rise, Tohoku earthquake

Devastating megathrust earthquakes and slow earthquakes both occur along subducting plate interfaces. These interplate seismic activities are strongly dependent on the nature of the plate interface, such as the shape of the plate interface and the materials and physical conditions along the plate interface. The oceanic plate, which is the input to the subduction zone, is the first order control on the nature of the plate interface. To reveal the nature of the subduction inputs to the northeastern Japan arc, we have conducted large-scale controlled-source seismic surveys of the northwestern part of the oceanic Pacific plate. The obtained seismic data have revealed (1) oceanic plate structural evolution caused by plate bending prior to subduction, suggesting the promotion of the oceanic plate hydration; (2) spatial variation of the oceanic plate structure, such as variations in the thickness of sediment and crust; (3) that the spatial variations are caused by both ancient plate formation processes and more recent volcanic activities; and (4) that spatial variations of the nature of the subduction inputs show good correlation with the along-strike variations in the seismic structure and seismic activities after subduction, including the coseismic slip distribution of the 2011 Tohoku earthquakes and the structural differences between the northern and the southern Japan Trench. These observations indicate that the incoming oceanic plate structure is much more spatially variable than previously thought and also imply that the spatial variation of the subduction inputs is a key controlling factor of the spatial variation of various processes in subduction zones, including interplate seismic activities and evolution of the forearc structure.

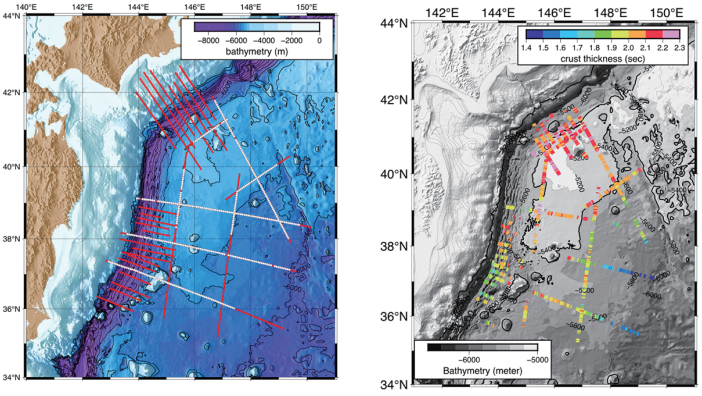

(left) Map of the study area. Red lines show multi-channel seismic (MCS) reflection survey lines and white circles represent Ocean Bottom Seismometers (OBSs) deployed along some of survey lines to obtain wide-angle seismic reflection and refraction data. (right) Map of the crustal thickness in two-way time derived from all the MCS lines, showing notable regional variations.

Published: 2023/8/22
https://doi.org/10.1186/s40645-023-00578-8

Progress in Earth and Planetary Science
https://progearthplanetsci.org/en/

Review articles : Solid earth sciences

Seismic noise between 0.003 Hz and 1.0 Hz and its classification

Toshiro Tanimoto, Aaron Anderson

Keywords: Low-frequency seismic noise, Ocean–solid earth interaction, Wave–wave interaction, Quasi-static deformation

It is now established that the primary microseism, the secondary microseisms, and the hum are the three main components of seismic noise in the frequency band from about 0.003 Hz to 1.0 Hz. Monthly averages of seismic noise are dominated by these signals in seismic noise. There are, however, some temporary additional signals in the same frequency band, such as signals from tropical cyclones (hurricanes and typhoons) in the ocean and on land, stormquakes, weather bombs, tornadoes, and wind-related atmospheric pressure loading. We review these effects, lasting only from a few hours to a week but are significant signals. We also attempt to classify all seismic noise. We point out that there are two broad types of seismic noise, the propagating seismic waves and the quasi-static deformations. The latter type is observed only for surface pressure changes at close distances. It has been known since about 1970 but has not been emphasized in recent literature. Recent data based on co-located pressure and seismic instruments clearly show its existence. Because the number of phenomena in the first type is large, we propose to classify all seismic noise into three categories: (1) propagating seismic waves from ocean sources, (2) propagating seismic waves from on-land sources, and (3) quasi-static deformation at ocean bottom and on land. The microseisms and the hum are in the first category although there are differences in the detailed processes of their excitation mechanisms. We will also classify temporary signals by these categories.

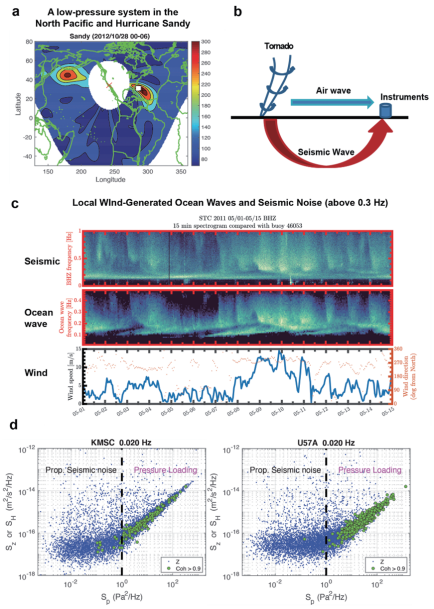

Figure:
(a) Beamforming for P-wave sources by an array analysis of the Southern California Seismic Network. There was a P-wave source near Hurricane Sandy when it (its center indicated by a white square) moved northward off the East coast of USA. In the same time interval, a low-pressure system in the northern Pacific Ocean was also emitting P waves. Body waves are often excited near a low-pressure system through the wave-wave interaction of ocean waves.
(b) Pressure inside a tornado is much lower than the ambient atmospheric pressure. When a tornado touches the Earth's surface, it acts as a single force because of this pressure difference and excites seismic waves. The excitation source strength, inverted from seismic data, matches the temporal variation of the Fujita scale determined for a tornado.
(c) In the frequency band 0.3-1.0 Hz, a slightly higher frequency band than the secondary microseism, we can see seismic noise caused by the wave-wave interaction of local ocean waves that in turn were generated by local winds. High amplitudes in seismic waves (top) and ocean waves (middle) are indicated by white and show close agreements in their temporal behavior. Wind speed (bottom) also shows a good correlation with ocean wave data, especially if we focused on high speed time intervals.
(d) Plot of vertical seismic PSD against pressure PSD allows us to separate the propagating seismic signals from distance sources and the loading ground deformation signals from local pressure sources. For pressure less than the one indicated by the vertical dashed line, the signals are propagating seismic waves from distant sources because their amplitudes are not affected by local pressure variations. For pressure higher than the dashed line, vertical seismic amplitudes increase with local pressure, indicating that they are generated by local surface pressure loading. Data from two EarthScope Transportable stations (KMSC, U57A) were used. Each point is from an analysis of 1-hour-long time series and the data were from the year 2014.

Published: 2023/9/11
https://doi.org/10.1186/s40645-023-00587-7

Progress in Earth and Planetary Science
https://progearthplanetsci.org/en/

Review articles : Solid earth sciences

An introductory review of the thermal structure of subduction zones: III—Comparison between models and observations

Peter E. van Keken, Cian R. Wilson

Keywords: Geodynamics, Plate tectonics, Finite element methods, Subduction zone metamorphism, Arc volcanism

The thermal structure of subduction zones is fundamental to our understanding of the physical and chemical processes that occur at active convergent plate margins. These include magma generation and related arc volcanism, shallow and deep seismicity, and metamorphic reactions that can release fluids. Computational models can predict the thermal structure to great numerical precision when models are fully described but this does not guarantee accuracy or applicability. In a trio of companion papers, the construction of thermal subduction zone models, their use in subduction zone studies, and their link to geophysical and geochemical observations are explored. In this last part, we discuss how independent finite element approaches predict the thermal structure of the global subduction system and investigate how well these predictions correspond to geophysical, geochemical, and petrological observations.

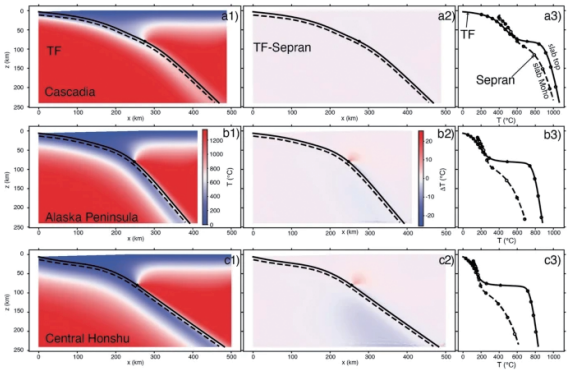

Comparison between TerraFERMA and Sepran predictions for the thermal structure of the models for Cascadia (row a), Alaska Peninsula (row b), and Central Honshu (row c). Column 1: Temperature as predicted by TerraFERMA. Slab top is indicated by the solid line and the slab Moho by the dashed line. Column 2: Temperature difference between predictions from TerraFERMA and Sepran. Slab top and Moho indicated as in column 1. Column 3: Comparison of the temperature at the slab top and slab Moho. Lines are from TerraFERMA (slab top solid lines, slab Moho dashed lines), open circles are from Sepran

Published: 2023/9/18
https://doi.org/10.1186/s40645-023-00589-5

Progress in Earth and Planetary Science
https://progearthplanetsci.org/en/

Review articles : Solid earth sciences

Recent progress in research on source processes of great earthquakes using tsunami data

Yuichiro Tanioka, Yusuke Yamanaka

Keywords: Research on source processes, Great earthquakes, Progress in tsunami research

This paper provides an overview of inverse studies that estimate earthquake source processes using tsunami-related data. Methods and techniques developed with those data associated with the 2004 Sumatra and 2011 Tohoku-oki earthquakes were reviewed. These events significantly impacted subsequent studies that focused on great historical earthquakes. Thus, recent advancements from studies on great historical earthquakes (M > 8) using old tsunami data, including documents and non-digital tsunami waveforms, have been reviewed. Another key earthquake was the 1700 Cascadia earthquake, and its source process was revealed using geological tsunami deposit data, which have led to a recent surge in prehistorical earthquake studies using tsunami deposit data. Considering this, the advancements in prehistorical earthquake studies have been reviewed. Finally, expected advancements in earthquake source process studies using tsunami-related data in the near future have been discussed.

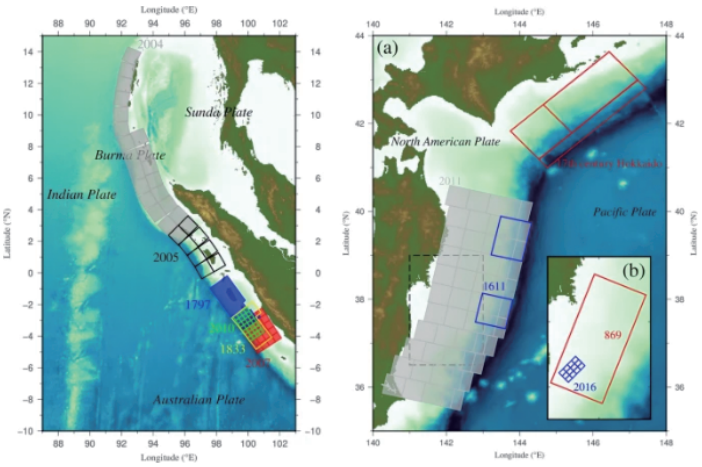

Sources of great earthquakes in Sumatra, Indonesia (left) and those in Northern Japan, off Hokkaido and Tohoku, (right) discussed in this paper.

Published: 2023/10/8
https://doi.org/10.1186/s40645-023-00593-9

Progress in Earth and Planetary Science
https://progearthplanetsci.org/en/

Review articles : Solid earth sciences

An introductory review of the thermal structure of subduction zones: II—numerical approach and validation

Cian R. Wilson, Peter E. van Keken

Keywords: Geodynamics, Plate tectonics, Finite element methods, Subduction zone metamorphism, Arc volcanism

The thermal structure of subduction zones is fundamental to our understanding of the physical and chemical processes that occur at active convergent plate margins. These include magma generation and related arc volcanism, shallow and deep seismicity, and metamorphic reactions that can release fluids. Computational models can predict the thermal structure to great numerical precision when models are fully described but this does not guarantee accuracy or applicability. In a trio of companion papers, the construction of thermal subduction zone models, their use in subduction zone studies, and their link to geophysical and geochemical observations are explored. In this part II, the finite element techniques that can be used to predict thermal structure are discussed in an introductory fashion along with their verification and validation.

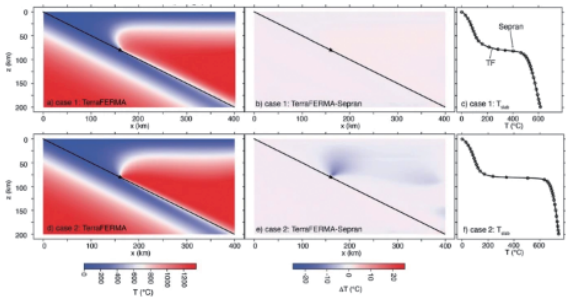

Steady-state thermal structure for the updated subduction zone benchmark. a) Temperature predicted by TF (TerraFERMA) for case 1 (constant viscosity h = 1); b) temperature difference between TF and Sepran using the penalty function (PF) method for case 1 at fm = 1 where fm represents the smallest element sizes in the finite element grids near the coupling point; c) slab top temperature comparison for case 1; and d)–f) as a)–c) but now for case 2 (temperature and strain rate dependent viscosity). The star indicates the position or temperature conditions at the coupling point.

Steady-state thermal structure for the updated subduction zone benchmark. a) Temperature predicted by TF for case 1; b) temperature difference between TF and Sepran using the penalty function (PF) method for case 1 at $f_m = 1$ where f_m represents the smallest element sizes in the finite element grids near the coupling point; c) slab top temperature comparison for case 1; and d)–f) as a)–c) but now for case 2. The star indicates the position or temperature conditions at the coupling point.

Published: 2023/11/30
https://doi.org/10.1186/s40645-023-00588-6

Progress in Earth and Planetary Science
https://progearthplanetsci.org/en/

Review articles : Solid earth sciences

Reconsideration of the energy balance in earthquake faulting

Mitsuhiro Matsu'ura

Keywords: Theoretical seismology, Background stress field, Earthquake faulting, Moment tensor, Inelastic strain, Elastic potential energy, Radiated seismic energy, Work done for shear faulting, Fault constitutive law, Rupture growth rate

The occurrence of earthquakes is now understood as brittle shear fracture releasing the elastic potential energy stored in the earth. Since the 1950s, many studies on the energy balance in earthquake faulting have been done, but there seems to be some incoherence among them. The essential reason is because various changes in conceptual framework happened during the last six decades, specifically the introduction of the new paradigm of plate tectonics in the 1960s, the concept of moment tensor as source representation in the 1970s, and the fault constitutive law governing rupture growth in the 1990s. Therefore, it will be worthwhile to reconsider the energetics of earthquake faulting from a current perspective. For this purpose, first of all, we summarize the basic concepts of elastic potential energy and moment tensor and review the general representation of earthquake sources and the origin of background crustal stress to confirm that the effect of earth's self-gravitation is negligible in the energetics of shear faulting. Next, as a starting point for discussion, we directly derive a basic equation of mechanical energy balance in dynamic shear faulting from the equation of motion for an elastic body subjected to tectonic-origin deviatoric stress. Then, we review the widely accepted formula for indirectly evaluating radiated seismic energy from a simplified energy balance equation and compare with the direct evaluation based on the analytical solution of displacement fields for a point dislocation source in order to call attention to inconsistency between them. The inconsistency comes from the omission of the effects of rupture growth rate in the simplified energy balance equation. So, finally, we review the energy balance at the tips of a propagating shear crack, which naturally leads to the introduction of the slip-weakening fault constitutive law as a fundamental equation governing earthquake rupture. Then, we discuss the whole process of earthquake rupture, consisting of initiation, acceleration, steady propagation, deceleration, and termination from the viewpoint of energy balance.

Difference in rupture growth path between dynamic faulting and aseismic slip:

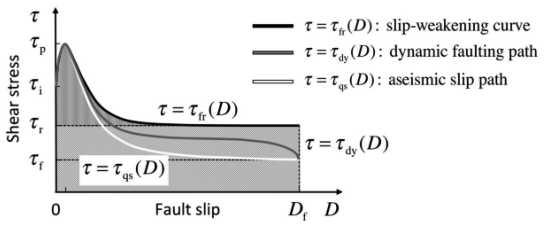

Total seismic energy escaping from the mechanical system:

$$-E_R/S = \int_0^{D_{final}} [\tau_{dy}(D) - \tau_{qs}(D)]\,dD$$

A schematic diagram showing the difference in rupture growth path between the dynamic and quasi-static cases. The thick gray curve $\tau = \tau_{dy}(D)$ and white curve $\tau = \tau_{qs}(D)$ represent the dynamic and quasi-static rupture growth paths, respectively. For reference, the slip-weakening curve $\tau = \tau_{fr}(D)$ is also plotted in black. The symbols τ_i, τ_p, τ_r, and τ_f indicate the initial, peak, residual, and final values of the shear stress τ, respectively. The dynamic rupture growth path is characterized by the initial slip-weakening phase, the intermediate high-speed rupture propagation phase, and the final slip deceleration and transient adjustment phase. The area enclosed by the thick gray and white curves, $\int_0^{D_{final}} [\tau_{dy}(D) - \tau_{qs}(D)]\,dD$, gives the total seismic energy escaping from the mechanical system concerned.

Published: 2024/1/9
https://doi.org/10.1186/s40645-023-00602-x

Progress in Earth and Planetary Science
https://progearthplanetsci.org/en/

Review articles : Solid earth sciences

Ambient noise multimode surface wave tomography

Kiwamu Nishida, Ryota Takagi, Akiko Takeo

Keywords: Ambient seismic noise, Multimode surface wave, Seismic interferometry, Surface wave tomography

Seismic techniques using earthquakes are powerful tools for exploring the Earth's internal structure. However, the earthquake distribution limits the spatial resolution. In recent years, ambient noise surface wave tomography using ambient seismic wave field has resolved these limitations. A typical ambient seismic wave field is microseisms excited by ocean swell activities. Ambient noise surface wave tomography is a technique in seismic interferometry that extracts seismic wave propagation between pairs of stations by cross-correlating the seismic records. The cross-correlation function can be interpreted as an impulsive response at a station with a virtual source at the other station. This technique became standard with the development of modern dense seismic networks. This paper reviews a theory of seismic interferometry for ambient noise surface wave tomography and procedures for practical data processing to calculate cross-correlation functions. The tomographic method typically consists of four steps: (1) the construction of reference 1-D models, (2) phase velocity measurements for each path, (3) 2-D phase velocity inversions, and (4) the construction of a 3-D S-wave tomographic model obtained from series of local 1-D inversions at all the grids. This paper presents the feasibility of multimode surface wave dispersion measurements for improving depth resolution.

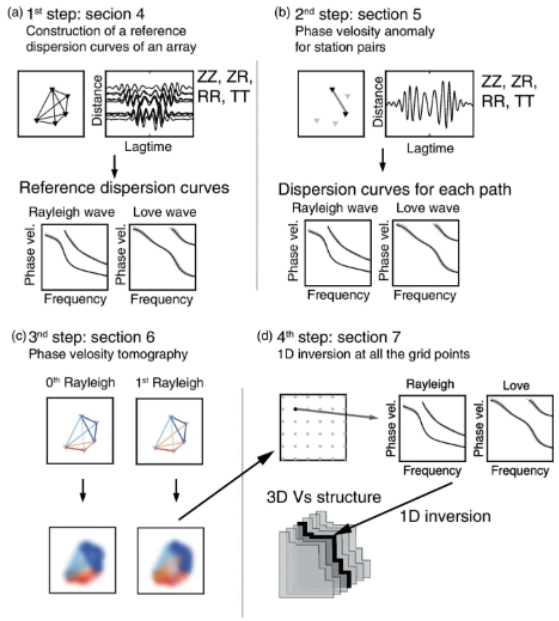

(a) Construction of reference 1-D models. (b) Phase/group velocity measurements for each path. (c) 2-D phase/group velocity inversions for multimodes. d A 3-D S-wave tomographic model is obtained from a collection of local 1-D inversions at all the grids. Modified from Takagi and Nishida (2022)

Published: 2024/2/8
https://doi.org/10.1186/s40645-023-00605-8

Progress in Earth and Planetary Science
https://progearthplanetsci.org/en/

Review articles : Solid earth sciences

Tectonic exhumation of a metamorphic core in an arc-continent collision during oblique convergence, Taiwan

Timothy Byrne, Michael Chojnacki, Jonathan Lewis, Jian-Cheng Lee, Gong-Ruei Ho, En-Chao Yeh, Yuan-Hsi Lee, Chin-Ho Tsai, Mark Evans, Laura Webb

Keywords: Exhumation, Arc-continent collisions, Ductile thinning, Extrusion, Taiwan

Observations over the last few decades from a number of orogenic systems have highlighted the possible importance of tectonic exhumation, i.e., ductile thinning and normal faulting, in exhuming rocks once buried in high-pressure conditions. Taiwan is one of the few active orogens in the world where rocks that once experienced high-pressure metamorphism (> 50 km) are exposed at the Earth's surface, providing a natural laboratory for advancing our understanding of exhumation processes. We integrate previously published studies of the Taiwan orogen with new structural, geochronological, and fluid inclusion microthermometry data to argue that tectonic extrusion and structural thinning played a critical role in exhuming the metamorphic core of the orogen until very recently, ca. 0.7 Ma. We propose a two-stage process for exhuming the high-pressure metamorphic rocks of the Yuli Belt: an initial stage where exhumation is driven primarily by pressure gradients in a subduction channel and a second stage that is initiated as an orogen-parallel regional-scale strike-slip zone, the Tailuko shear zone, is offset by an orogen-normal strike-slip zone. The offset generates an extensional bend that is filled with extruding high-pressure rocks as the upper crust is structurally thinned. Evidence for tectonic thinning comes primarily from a low-angle penetrative foliation that records significant vertical shortening and a suite of sub-vertical late-stage, mineral-filled veins. Isotopic dating indicates that the second stage started ca. 2.4–3.1 Ma and ended at ca. 0.7 Ma when the northern Backbone Range orocline started to form. We propose the low-angle foliation formed in the footwall of a regional-scale extensional shear zone that rooted to the east, beneath the forearc. Combined tectonic and erosional processes may have limited the topographic growth of the orogen from ~3.0 to < 1.0 Ma.

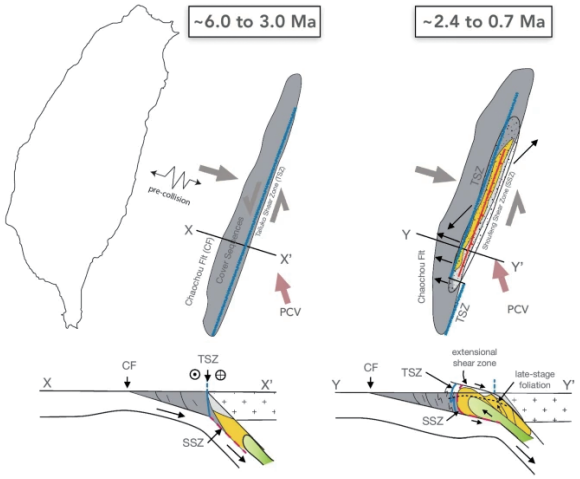

Subduction and accretion of trench sediments (light grey, yellow) and initial extrusion of the mantle (~6Ma to 3Ma). Forceful extrusion of subducted materials (light grey, yellow, green) (~2.4Ma to 0.7Ma). Extrusion offsets TSZ (Tailuko Shear Zone), forming a releasing bend, and is accommodated by motion along the Chaochou thrust and an extensional shear zone.

Published: 2024/4/17
https://doi.org/10.1186/s40645-024-00627-w

Progress in Earth and Planetary Science
https://progearthplanetsci.org/en/

Review articles : Solid earth sciences

Review of experimental and analytical techniques to determine H, C, N, and S solubility and metal–silicate partitioning during planetary differentiation

Celia Dalou, Terry-Ann Suer, Laurent Tissandier, Weronika L. Ofierska, Alice Girani, Paolo A. Sossi

Keywords: Differentiation, Magma ocean, Core formation, Evaporation, Experimental techniques, Low-pressure, High-pressure, Oxygen fugacity, Analytical techniques, Partition coefficients

During their formation, terrestrial planets underwent a magma ocean phase during which their metallic cores segregated from their silicate mantles and their early atmospheres formed. These planetary formation processes resulted in a redistribution of the abundances of highly volatile elements (HVEs, such as H, C, N, and S) between the planets' metallic cores, silicate mantles, and atmospheres. This review presents the numerous experimental techniques used to simulate the conditions and identify the parameters that influenced the behavior of HVEs during planetary formation. We also review the analytical techniques used to characterize the different types of experimental samples and quantify the distribution of HVEs between metallic and silicate phases, as well as their solubilities in silicate glasses. This exhaustive review targets students and young researchers beginning their work on the subject, or, more generally, scientists seeking a better understanding of this field of research.

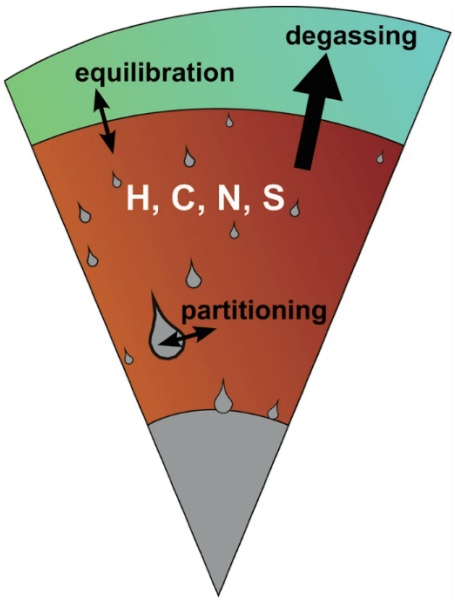

Published: 2024/5/7
https://doi.org/10.1186/s40645-024-00629-8

Progress in Earth and Planetary Science
https://progearthplanetsci.org/en/

Review articles : Solid earth sciences

Cenozoic history of the Australian Monsoon

Stephen J. Gallagher, Vera A. Korasidis, Gerald Auer, David De Vleeschouwer, Jeroen Groeneveld and Beth Christensen

Keywords: Paleomonsoon, Pseudo-Monsoon, Quasi-Monsoon, Cenozoic, Quaternary, Proxies

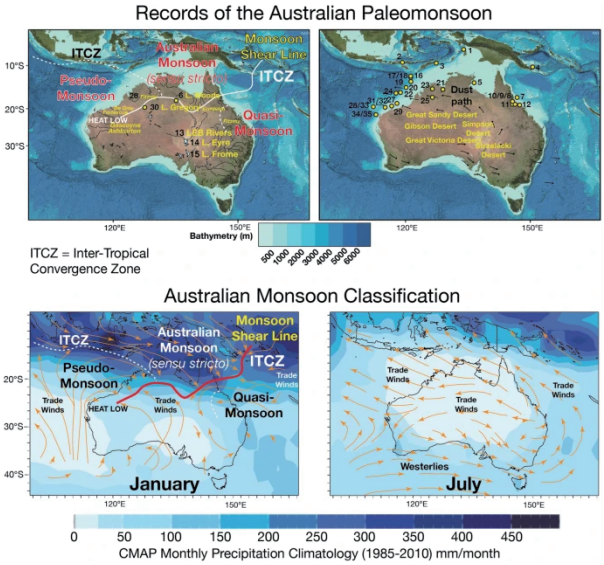

The Australian monsoon is part of the global monsoon and often included as a component of the Asian Monsoon system although they operate out of phase. Due to their hemispheric positions, the dry (wet) Australian winter (summer) monsoon coincides with the wet summer Asian monsoon and vice versa. The Australian monsoon controls rainfall distribution in northern tropical Australia where over 80% of the median annular rainfall occurs from December to March, the summer wet season. Three types of the Australian monsoon are distinguished based on distinct atmospheric circulation and heating patterns: a northwest Pseudo-Monsoon, a northeast Quasi-Monsoon and an Australian Monsoon (sensu stricto) north of Australia. While the modern climatology of the Australian monsoon has been extensively documented, its paleohistory is poorly constrained, especially in Australia's continental interior where harsh arid climatic conditions have degraded almost all physical evidence of monsoonal activity. However, reassessment of northern and central Australian terrestrial and marine sequences reveals a fairly robust Cenozoic history of this monsoon, especially for the Neogene, which we synthesize for the first time here. Evidence for a Paleogene Australian paleomonsoon is equivocal due to the small number of sites, their limited age control, and the poor preservation of flora with ambiguous affinities. Modeling and tectonic evidence suggest the northern part of the Australian Plate migrated to the (sub) tropical region (north of 30°S) creating "modern" boundary conditions for monsoonal onset by ~10 Ma. Cores off northwest Australia reveal arid late Miocene and humid Pliocene conditions were followed by the Pseudo-Monsoon at ~3.5 Ma when northern hemisphere glacial expansion "forced" the ITCZ (Inter Tropical Convergent Zone) south. Subsequently, variable humid and arid periods typify Quaternary high-amplitude glacio-eustatic cycles until ~1 Ma, when arid conditions expanded across Australia. Glacial/interglacial cyclicity and obliquity/precession insolation during terminations modulated Pseudo-Monsoon intensity when the ITCZ migrated northward (during glacial) and southward (during interglacial periods) from ~1 Ma to present. From ~1.6 to 1 Ma, precession paced Pseudo-Monsoon variability. Mega-lake expansion in central Australia and fluvial intensification generally correspond to wetter interglacial periods. Lake Eyre monsoonal shorelines may have been influenced by abrupt millennial events. Monsoonal conditions re-established near the base of Holocene as the ITCZ migrated across northern Australia. The Australian Monsoon (sensu stricto) and Quasi-Monsoon (a) initiated from 12.5 to 11 ka; (b) intensifying from 9 to 2 ka; then (c) weakened, possibly due to the onset of ENSO intensification. The Pseudo-Monsoon was established at ~14.5 ka off northwest Australia intensifying from 11.5 to 7 ka. It weakened after ~7 ka north of 15°S and ~5 ka to the south. In the absence of a topographic influence, insolation (precession/obliquity), abrupt millennial events and/or ITCZ variability across northern Australia were important controls on Quaternary Australian monsoon intensity. Further investigations of deeper time pre-Quaternary records off northwest and northeast Australia will reveal the paleohistory of this important domain of the Global Monsoon.

Published: 2024/11/21
https://doi.org/10.1186/s40645-024-00662-7

Progress in Earth and Planetary Science
https://progearthplanetsci.org/en/

Review articles : Solid earth sciences

Role of water in dynamics of slabs and surrounding mantle

Eiji Ohtani, Takayuki Ishii

Keywords: Water partitioning, NAMs, DHMS, Hydration, Dehydration, Slabs, Fluid, Seismic scatterers, Intermediate-depth earthquakes, Deep-focus earthquakes

Water bound to various hydrous minerals can be transported deep into the mantle by slab subduction. Serpentine is one of most important hydrous minerals in the crust and shallow upper mantle. A partially serpentinized slab mantle limits the amount of water that can enter deep into the mantle. The partitioning of water between hydrous minerals and nominally anhydrous minerals (NAMs) is a crucial factor in controlling the physical properties and dynamics of slabs. Recent experiments on water partitioning have revealed that water strongly partitions to coexisting hydrous minerals. NAMs, such as olivine and its high-pressure polymorphs, have limited water content in water-undersaturated wet slabs. Metastable olivine wedges are not a feature of dry slabs, but can be of wet slabs that are not saturated with water. The transformation kinetics of the dry state, which generates deep-focus earthquakes and produces significant deformation in the slab, can work under wet slabs. Water bound to hydrous minerals is transported by the slab to the mantle transition zone and lower mantle. Hydrous minerals in stagnant slabs over 660 km depth release water as the slab warms, producing locally hydrated mantle transition zones and dense water-bearing magmas at the base of the upper mantle, and generating intraplate volcanism, which are referred to as the big mantle wedge model. Seismic scatterers are observed in the lower mantle at depths from 700 to 1900 km. These scatterers may be caused by water release at the top of the lower mantle by dehydration of hydrous minerals such as dense hydrous magnesium silicates. The shear instability due to the second order phase transformation from stishovite to CaCl2-type phase in hydrous aluminous SiO2 also causes the depth variation of seismic scatterers in the lower mantle. The high-pressure polymorphs of aluminous SiO2 contain a large amount of water more than 1 wt%, which can be important water carriers under lower mantle conditions.

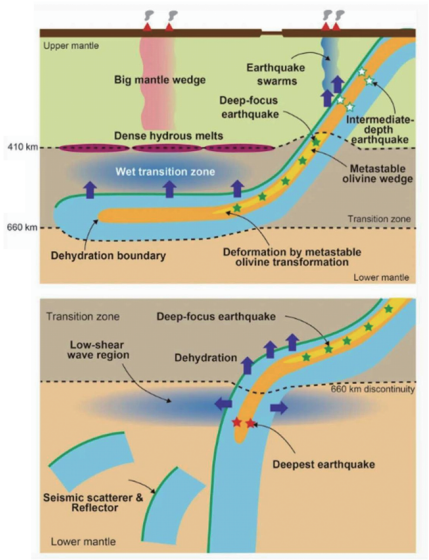

Processes associated with slab dehydration in the deep mantle. (A) The release of water through the decomposition of hydrous minerals of the slabs in the upper mantle produces earthquake swarms in the mantle wedge above the slab. Olivine may remain metastable to the transition zone depths in “wet” slabs, because water partitions into dense hydrous magnesium silicates resulting in formation of dry olivine. (B) Seismic reflectors and scatterers in the lower mantle may be created by fluids or melts released from the slabs due to decomposition of DHMSs (Dense Hydrous Magnesium Silicates) or the stisohivite-CaCl2-type silica transformation of the hydrous SiO2 phase in the basalt layer of the slab descending into the lower mantle.

Published: 2024/12/13
https://doi.org/10.1186/s40645-024-00670-7

Progress in Earth and Planetary Science
https://progearthplanetsci.org/en/

Review articles : Solid earth sciences

Rheology of the lower mantle: a review

Shun-ichiro Karato, Jennifer Girard, Heechen E. Cho

We review our current understanding of the rheological properties of the lower mantle based both on materials science and geophysics points of view. We assume a simple model of the lower mantle that is made of only two minerals: bridgmanite (Br) (Mg,Fe)SiO3 and ferropericlase (Fp) (Mg,Fe)O, and address a question of (i) which mineral is weaker (lower viscosity), (ii) how does lower mantle viscosity change with depth and location, and (iii) discuss implications for shear localization. We first review plausible mechanisms of deformation based on the deformation mechanism map on the normalized stress and temperature space. We conclude that likely mechanism of deformation in the lower mantle is either diffusion creep or power-law dislocation creep. Based on this review, we discuss recently proposed models by Cordier and his group (Cordier in Nature 481:177–181, 2012; Cordier in Nature 613:303–306 , 2023) where either asthermal creep (i.e., low-temperature plasticity) or pure climb creep (not power-law dislocation creep) would play an important role. We conclude that these models are not acceptable because (1) many aspects of their models are incompatible with experimental observations and theoretical models of deformation of most materials including oxides and metals and (2) these models are not consistent with the distribution of seismic anisotropy. Hence, we focus on power-law dislocation creep and diffusion creep. We review previously published results on deformation (by dislocation creep) and diffusion, we conclude that Fp is weaker than Br. The radial (depth) depth and lateral variation of viscosity is discussed based on the estimated activation volume and estimated variation of grain-size. Geophysical studies suggest only modest depth variation of viscosity that demands relatively small activation volume (V* (<3 × 10–6 m3/mol)). Plausible models to explain small activation volume are discussed including the role of extrinsic diffusion. Grain-size also controls viscosity if deformation is by diffusion creep. Okamoto and Hiraga (J Geophys Res, 2024. 10.1029/2023JB027803), Solomatov et al. (Phys Earth Planet Inter 129:265–282, 2002) estimated the grain-size evolution in the lower mantle based on the kinetics of grain-growth and the role of a phase transformation. In contrast, there are other papers (e.g., Paul et al. in Prog Earth Planet Sci 11:64, 2024; Rozel in Geochem Geophys Geosyst, 2012. 10.1029/2012GC004282) where grain-size distribution is estimated assuming that grain-size is controlled by dynamic recrystallization. The validity of assumption is questionable because dynamic recrystallization occurs due to deformation by dislocation creep but not by diffusion creep and the absence of seismic anisotropy indicates that diffusion creep dominates in most of the lower mantle. Finally, we review the published models of shear localization that would explain the long-term preservation of geochemical reservoirs in the lower mantle. Accepting that two minerals (Fp and Br) in the lower mantle have largely different viscosity, Ballmer et al. (Nat Geosci 10:236–240, 2017) proposed that the presence of regions of compositional difference (difference in Fp/Br ratio) leads to localized deformation (deformation mainly in the weaker regions). However, in addition to the ad hoc nature of this model, there is no strong evidence for the presence of large variation in Fp/Br in the lower mantle that makes the validity of this model questionable. There are some papers where processes of shear localization are explored without invoking the presence of regions of large rheological contrast. Thielmann et al. (Geochem Geophys Geosyst, 2020. 10.1029/2019GC008688) presented the results of theoretical study of deformation of initially homogeneous two-phase mixture (Fp and Br) and showed that deformation causes the elongation of a weak Fp that promotes shear localization. In this model, the rheological contrast between Fp and Br was assumed to be independent of strain. However, Cho and Karato (J Geophys Res 2022. 10.1029/2021JB022673 ; Phys Earth Planet Inter, 2024. 10.1016/j.pepi.2024) showed that when deformation is by diffusion creep, the rheological contrast increases with strain due to the evolution of stress concentration caused by grain elongation. They showed that this will promote strain weakening particularly in simple shear that would lead to shear localization. Consequently, the tendency for shear localization is stronger in their model than a model where rheological contrast is assumed to be independent of strain.

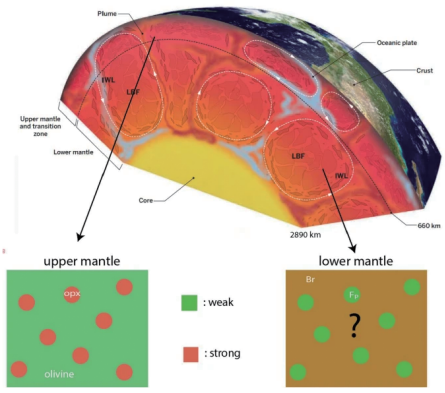

Published: 2025/03/25
https://doi.org/10.1186/s40645-025-00695-6

Progress in Earth and Planetary Science
https://progearthplanetsci.org/en/

Review articles : Biogeosciences

Accessing the energy-limited and sparsely populated deep biosphere: achievements and ongoing challenges of available technologies

Yuki Morono

Keywords: Subseafloor biosphere, Low energy habitat, Technical developments, Limits of life

Microbes in marine sediments detected and counted by direct observation of membrane-filtered sediment samples stained with acridine orange. This technique can still be applied to high-biomass ($>10^5$ cells/cm^3) sedimentary habitats, such as organic-rich sediments collected in shallow areas near the seafloor. However, to further explore the nutrients and energy turnover under extremely low energy flux conditions, or in habitats that are close to the lower limit of the biosphere, technological breakthroughs have been required to increase the detection sensitivity for microbial life at densities of a few cells/cm^3 of sediment. These technological developments contributed to increasing fundamental information on microbial life at the fringes of the subseafloor biosphere and led to the discovery of revivable microbes in sediments aged up to 101.5 million years old. More recently, chemical detection methods have revealed the existence of spores in the deep biosphere that are impermeable to conventional DNA stains. Previous applications of molecular biology-based approaches have been limited to relatively higher biomass samples, potentially because the cells surviving in these very low energy flux environments have less integrated genomes. Here, I review the contribution and importance of the technological developments that have been made in the study of microbes from the subseafloor biosphere, recent developments of alternative methods to microscopically detect microbial spores and their application to deep subseafloor sediments, and the challenges associated with applying molecular biological approaches to study low-biomass samples.

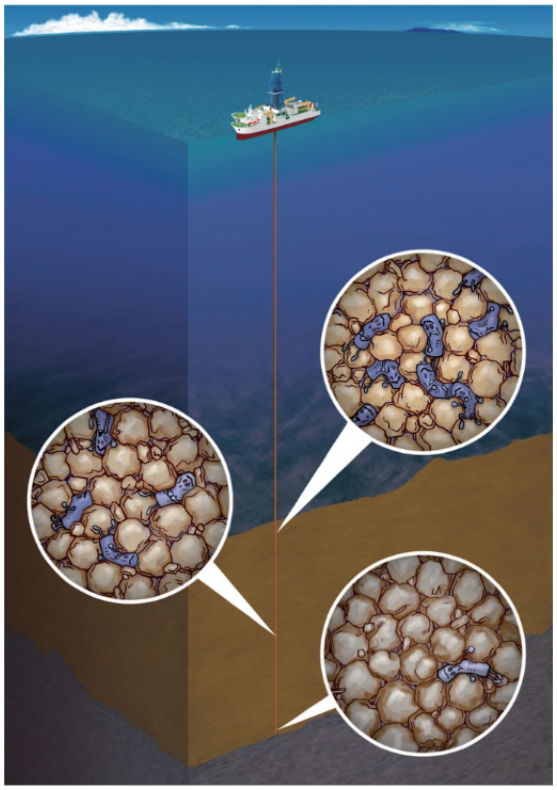

Cartoon diagram of the subseafloor biosphere. The increasing challenges for the survival of microbes are illustrated toward the depth of subseafloor.

Published: 2023/4/10
https://doi.org/10.1186/s40645-023-00551-5

Progress in Earth and Planetary Science
https://progearthplanetsci.org/en/

Review articles : Biogeosciences

Geological history of the land area between Okinawa Jima and Miyako Jima of the Ryukyu Islands, Japan, and its phylogeographical significance for the terrestrial organisms of these and adjacent islands

Watanabe N, Arai K, Otsubo M, Toda M, Tominaga A, Chiyonobu S, Sato T, Ikeda T, Takahashi A, Ota H, Iryu Y

Keywords: Ryukyu Islands, Kerama gap, Okinawa–Miyako submarine plateau, Pleistocene, Shimajiri Group, Ryukyu Group, Vertebrate, Phylogeography, OMSP hypothesis

The modern and Late Pleistocene terrestrial fauna of Miyako Jima and adjacent islands (the Miyako Islands) in the southern Ryukyu Islands, southwestern Japan, includes some endemic taxa or genetically unique populations that exclusively have closest allies in the more isolated Okinawa Jima and adjacent islands (the Okinawa Islands) than in the Yaeyama Islands, which are located southwest of the Miyako Islands with much narrower intervening straits. Those taxa or populations include representatives of lineages that have physiologically highly limited ability for over-sea dispersal and the Miyako Islands are currently separated from the Okinawa Islands by at least 300 km of open water; therefore, the formation of this phylogeographical pattern is perplexing. In this study, we review the late Cenozoic geology of the Miyako Islands, southern Okinawa Jima, the Okinawa–Miyako submarine plateau (OMSP; a plateau located between Okinawa Jima and Miyako Jima), and the Kerama gap, which is a depression between the OMSP and Okinawa Jima. We then consider the origin of the modern and Late Pleistocene terrestrial animals, including a number of non-volant vertebrates on the Miyako Islands. Finally, we propose a new hypothesis (the OMSP hypothesis) to explain the enigmatic composition of modern and Late Pleistocene terrestrial vertebrate fauna of the islands. Southern Okinawa Jima was uplifted and emerged after ca. 2 Ma and was temporarily connected to the OMSP, which is likely to have emerged earlier than southern Okinawa Jima, to form a large island extending from Okinawa Jima to the Miyako Islands with a NE–SW direction of ~ 400 km. Subsequently, Okinawa Jima became separated from the OMSP when the Ryukyu Group—which is composed of Quaternary reef and associated fore-reef and shelf deposits—began to accumulate around the island at 1.7–1.4 Ma. During the interval from 2.0 to 1.7–1.4 Ma, numerous terrestrial animals, including flightless vertebrates, extended their distribution to the OMSP. Although the Miyako Islands repeatedly underwent complete submergence during deposition of the main part of the Ryukyu Group (1.25–0.4 Ma), they were uplifted and emerged to become a land area after ca. 0.4 Ma. In contrast, the OMSP subsided after ca. 0.4 Ma and was almost completely submerged after 0.27 Ma. During ca. 0.4–0.27 Ma, terrestrial animals migrated from the OMSP to the Miyako Islands.

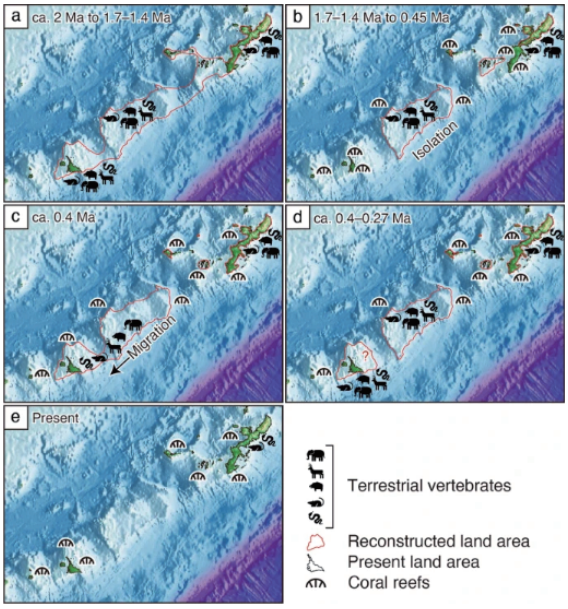

Changes in the paleogeography of the Okinawa–Miyako area and migration of terrestrial vertebrates. 1. a Period from after deposition of the Shimajiri Group to before deposition of the Ryukyu Group (ca. 2 to 1.7–1.4 Ma). b Period of interglacial highstands of sea level during deposition of the main body of the Ryukyu Group (1.7–1.4 to 0.45 Ma). Note that reef formation started significantly later on the Miyako Islands (1.25 Ma on Irabu Jima and 0.96 Ma on Miyako Jima) than on Okinawa Jima (1.7–1.4 Ma). c Period immediately after deposition of the main body of the Ryukyu Group (ca. 0.4 Ma). d Period after deposition of the main body of the Ryukyu Group (ca. 0.4–0.27 Ma). The OMSP was almost completely submerged after 0.27 Ma. e Present.

Published: 2023/7/20
https://doi.org/10.1186/s40645-023-00567-x

Progress in Earth and Planetary Science
https://progearthplanetsci.org/en/

Review articles : Interdisciplinary research

Review of radiolarian microfossils as a tool for reconstructing sea surface temperature of the past in the Northwest Pacific

Kenji M. Matsuzaki, Takuya Itaki, Yoshimi Kubota, Kyung Eun Lee, Isao Motoyama, Takuya Sagawa, Keiji Horikawa, Masafumi Murayama, Hajime Obata

Keywords: Radiolarian, Sea surface temperature (SST), Radiolarian-based SSTs, G. ruber Mg/Ca-based SSTs, Alkenone-based SSTs, Northwest Pacific, Water masses

In this review we re-evaluated the potential of radiolarian species as palaeoceanographic proxies in the Northwest Pacific Ocean relying on 33 new samples collected since 2021, combined with already published datasets. Our re-evaluation revealed significant differences between Sea of Japan and Northwest Pacific radiolarian assemblages, leading to the exclusion of the Sea of Japan dataset for further sea surface temperature (SST) reconstructions in the Northwest Pacific. By employing factor analyses, we were able to identify four distinct radiolarian assemblages characterizing the Northwest Pacific and East China Sea as follows: the Subtropical, the Sea of Okhotsk-related subarctic, the Oyashio Current to transitional zone-related, and the coastal water assemblages. Each assemblage showed specific species associations with different water masses and SST ranges. Species like Tetrapyle circularis/fruticosa and Dictyocoryne tetrathalamus were associated with waters above 24 °C, while Lithomelissa setosa and Ceratospyris borealis were associated temperatures below 14 °C. Based on a review of the literature about modern radiolarian species blooming conditions in the Northwest Pacific, we suggest that radiolarian species-based reconstructed SSTs more likely infer summer SSTs. Applying weighted averaging partial least squares transfer function on selected radiolarian species showing strong affinities with changes in summer SST, we re-evaluated past summer SSTs at IODP Site U1429 in the northern East China Sea with high accuracy (R2 = 0.97, error margin ± 1.4 °C). Our radiolarian-based summer SST reconstruction is similar to Globigerinoides ruber Mg/Ca-based summer SSTs, though showing minor disparities during glacial periods, while constant disparities were observed with alkenone-based SST estimates at the same site, which is likely due to seasonal biases. Notably, we identified L. setosa as a potential proxy for East Asian Winter Monsoon intensity.

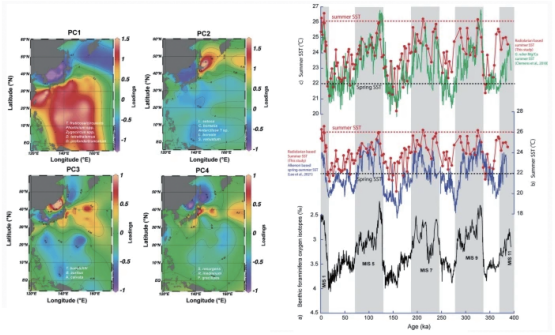

Published: 2025/5/19
https://doi.org/10.1186/s40645-025-00706-6

Date of Issue : March, 2026

Correspondence: peps_edit@jpgu.org

PEPS is supported by a Grant-in-Aid for Publication of Scientific Research Results (25HP2004) from Japan Society for the Promotion of Science.